УДК 624.154.9

Hyunho Shin, Ph.D.
Dong-Bin Jeong, Ph.D.
Gangneung-Wonju National University, Gangneung, Republic of Korea
Jong-Bong Kim, Ph.D.
Seoul National University of Technology, Seoul, Republic of Korea
Yo-Han Yoo, Ph.D.
Agency for Defense Development, Daejeon, Republic of Korea

A NUMERICAL STUDY ON THE EFFECT OF END RESTRAINT OF SPECIMEN IN CONVENTIONAL TRIAXIAL TEST ON THE YIELD STRENGTH AND THE POST-YIELD BEHAVIOR OF SOIL

The effects of end restraint in a conventional triaxial test on yield strength and the post-yield behavior of soil have been investigated by way of a finite element analysis based on a pressure-dependent and linearly elastic-perfectly plastic constitutive model. The influence of end restraint on the yield strength is insignificant. Unlike the yield strength, post-yield behavior is influenced notably by the end restraint, depending on the confinement pressure. When the axial and radial strains are small, strain hardening after initial yielding generally takes place. As the strain increases further, peak stress appears, followed by strain softening thereafter. As the confinement pressure increases, the peak stress materializes at lowered axial and radial strains, so that from the confinement pressure of 50 psi (344.7 kPa), strain softening starts almost from the initial yielding. As the confinement pressure increases, the degrees of strain hardening by the end restraint at the given axial and radial strains show decreasing trends. This change in yield strength as well as the artificial post-yield behavior (strain hardening or softening) due to the end restraint need to be eliminated in order to extract a true soil property from the triaxial stress-strain curve.

Keywords: *conventional triaxial test, end restraint, yield strength, post yield behavior, soil and crushable foam model, finite element analysis.*

Хюнго Шін, к.т.н.
Донг-Бін Джонг, к.т.н.
Кванджуський національний університет, Республіка Корея
Джонг-Бонг Кім, к.т.н.
Сеульський національний технологічний університет, Сеул, Республіка Корея
Йо-Хан Хйо, к.т.н.
Агентство з розвитку оборони, Дечон, Республіка Корея

ЧИСЕЛЬНЕ ДОСЛІДЖЕННЯ ЕФЕКТУ КРАЙОВИХ ОБМЕЖЕНЬ ДЕФОРМАЦІЙ ЗРАЗКІВ ПРИ СТАНДАРТНИХ ТРЬОХОСЬОВИХ ВИПРОБОВУВАННЯХ НА МЕЖІ ТЕКУЧОСТІ ТА ПІСЛЯ ТЕКУЧОЇ ПОВЕДІНКИ ҐРУНТУ

Ефекти крайових обмежень у стандартних трьохосьових випробовуваннях на межі текучості та після стадії текучої поведінки ґрунту досліджено за допомогою скінченно-елементного аналізу, що базувався на залежності між тиском і пружно-ідеально-пластичною континуальною моделлю. Вплив крайових обмежень на межі текучості незначний. На відміну від поведінки зразка ґрунту на межі текучості, на стан після неї впливають особливості крайових обмежень, що залежать від величини тиску. Коли осьові та радіальні деформації малі, то, як правило, після початку текучості відбуваються деформації зміцнення. При збільшенні деформацій з'являється пікове напруження, після чого відбувається руйнування зразка. При подальшому збільшенні тиску пікове

напруження зменшується при зниженні осьових і радіальних деформацій так, що при кінцевому тискові в 50 фунтів на квадратний дюйм (344,7 кПа) деформації руйнування починаються мало не з початку межі текучості. При подальшому зростанні тиску ступінь деформацій зміцнення до крайових обмежень на цих осьових і радіальних деформаціях має тенденції до зниження. Ця зміна межі текучості, а також штучна поведінка після межі текучості (деформації зміцнення чи руйнування) у зв'язку з крайовими обмеженнями мають бути усунуті, щоб правильно визначати властивості ґрунтів за кривою «напруження – деформації» при трьохосьових випробовуваннях.

Ключові слова: *трьохосьові випробовування, крайове обмеження, межа текучості, поведінка після текучості, ґрунтова модель і модель руйнування, скінченно-елементний аналіз.*

Хюнго Шин, к.т.н. Донг-Бин Джонг, к.т.н
Кванджуский национальный университет, Канвондо, Республика Корея
Джонг-Бонг Ким, к.т.н.
Сеульский национальный технологический университет, Сеул, Республика Корея
Йо-Хан Хйо, к.т.н.
Агентство по развитию обороны, Дечон, Республика Корея

ЧИСЛЕННОЕ ИССЛЕДОВАНИЕ ЕФФЕКТА КРАЕВЫХ ОГРАНИЧЕНИЙ ДЕФОРМАЦИЙ ОБРАЗЦОВ ПРИ СТАНДАРТНЫХ ТРЁХОСНЫХ ИСПЫТАНИЯХ НА ПРЕДЕЛЕ ТЕКУЧЕСТИ И ПОСЛЕ ТЕКУЧЕГО ПОВЕДЕНИЯ ГРУНТА

Эффекты краевых ограничений в стандартных трёхосных испытаниях на пределе текучести и после стадии текучего поведения грунта исследованы с помощью конечно-элементного анализа, который базируется на зависимости между давлением и упруго-идеально-пластической континуальной моделью. Влияние краевых ограничений на пределе текучести незначительное. В отличие от поведения образца грунта на пределе текучести, на его состояние после влияют особенности краевых ограничений, которые зависят от величины давления. Когда осевые и радиальные деформации малы, то, как правило, после начала текучести происходят деформации упрочнения. При увеличении деформаций появляются пиковые напряжения, после чего происходит разрушение образца. При дальнейшем увеличении давления пиковые напряжения уменьшаются при понижении осевых и радиальных деформаций так, что при конечном давлении в 50 фунтов на квадратный дюйм (344,7 кПа) деформации разрушения начинаются чуть ли не с начала предела текучести. При дальнейшем возрастании давления степень деформаций упрочнения до краевых ограничений на данных осевых и радиальных деформациях имеют тенденцию к снижению. Это изменение предела текучести, а также искусственное поведение после предела текучести (деформации упрочнения или разрушения) в связи с краевыми ограничениями должны быть устранены, чтобы правильно определять свойства грунтов по кривой «напряжения – деформации» при трёхосных испытаниях.

Ключевые слова: *трёхосные испытания, краевое ограничение, предел текучести, поведение после текучести, грунтовая модель и модель разрушения, конечно-элементный анализ.*

Introduction. The determination of the mechanical properties of soils has probably been most widely carried out by way of the conventional triaxial test. In this test, the soil specimen is assumed to deform uniformly, and the axial stress and two radial stresses are the three principal stresses. Thus, the

information obtained from the test is assumed to represent the true material properties of the tested soil. According to Bishop and Henkel [1], Taylor reported in 1941 that no significant error occurred in the measurement of soil strength when the length-to-diameter ratio of the triaxial specimen was in the range of 1.5-2.5.

However, an end restraint, which is caused by the friction between the top/bottom ends of the soil specimen and supports, exists in the specimen. The end restraint is amplified by the attachment of a rubber membrane to the end supports. It is well documented that the end restraint yields a non-uniform deformation of specimen (barreling) during a triaxial test [2-4]. Schanz and Gussman [2] reported that the shear strength of an idealized elastic-perfectly plastic triaxial specimen increased with an increasing end restraint and was not significantly influenced by the specimen geometry. In a numerical investigation by Sheng *et al.* [3], the end restraint caused the barrel-shaped deformation of the specimen, while non-uniformity in stress and strain increased with increasing strain. The non-uniformity of stress and strain in the triaxial specimen due to the end restraint was also well illustrated in the numerical study of Yang and Ge [3]. Thus, the stress-strain curve determined by the conventional triaxial test, strains of which are determined based on the positions of the end cap and radial ends, inevitably includes the artificial behavior caused by the non-uniform deformation in addition to the true material behavior.

Although the importance and degree of non-uniformity in strain and stress in the interior of the specimen during the triaxial test have been well illustrated in existing studies, to our knowledge, numerical studies simulating a stress-strain curve following the experimental procedure, i.e. the determination of strains based on the positions of the top end and radial ends of the specimen, have thus far been few. In this regard, the current study, through a finite element analysis, numerically investigates how the triaxial stress-strain curve based on an experimental procedure is influenced by the presence of the end restraint. The present study was carried out by employing a pressure-dependent and linearly elastic-perfectly plastic constitutive model.

Constitutive model. The employed constitutive model in the current investigation is the soil and crushable foam (SCF) model [5, 6] which is a pressure-dependent and linearly elastic-perfectly plastic model for geomaterials. In this model, the yield function describes the pressure-dependent deviatoric deformation of geomaterials by the relation,

$$J_{2D} = a_o + a_1 p + a_2 p^2 \ , \qquad (1)$$

where J_{2D} is the second deviatoric stress invariant, p is the pressure, and a_0, a_1, and a_2 are the material parameters to be determined by experimentation. This model is one of the most basic constitutive models used for describing the plasticity of geomaterials. Thus, it has accumulated a considerable amount of user experience and feedback, and it is also quite robust [7]. The SCF model has found wide application areas in the numerical simulations of versatile soil-

structure interactions [8-10]. It is now implemented in commercial finite element packages, such as LS-DYNA [11] and MSC DYTRAN [12].

Numerical analysis. The present investigation analyzes half of the 2D axisymmetric space (Fig. 1). The modeled size of the radial x-y plane of the specimen was 0.75 inch (19.05 mm) in radius and 3.0 inches (76.2 mm) in height. The thickness of the rubber membrane was 7.874 milli-inches (0.2 mm). The model areas were discretized by using 4-node axisymmetric quadratic elements. The number of elements was 50, and the size of the elements was checked by a separate mesh quality test.

For the simulation of the ideal case with no end restraint, the nodes at the top end of the specimen were allowed to move freely along the axial (y-axis) and radial (x-axis) directions, while the movement of the nodes at the bottom end was allowed only along the radial direction. For the simulation of the case with an end restraint, the nodes at the top end of the specimen were allowed to move only along the axial direction, while the movement of the nodes at the bottom end was fixed along all directions. For both cases, the nodes at the bottom of the specimen were allowed to move only along the radial direction.

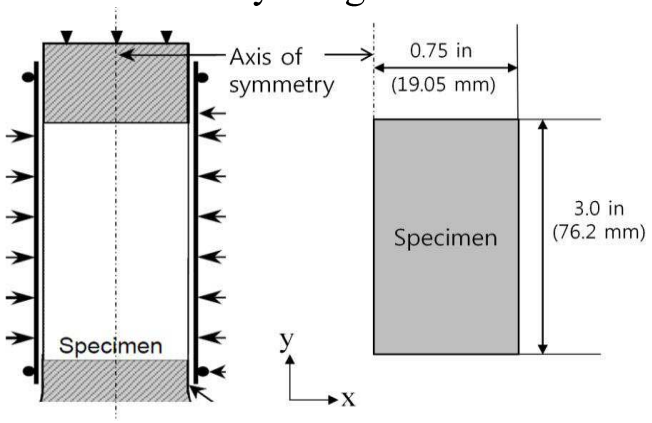

Fig. 1. Schematic illustration of the model for finite element analysis

The right (circumferential) boundary was subjected to constant radial pressures of 2, 5, 10, 20, 50 and 70 psi (13.8, 34.5, 68.9,137.9, 344.7 and 551.6 kPa), which were equal to the confinement pressures. In order to realize the hydrostatic loading condition, the radial pressure was applied first, followed by the application of the axial stress until it reached the radial pressure via the control of the axial displacement of nodes located at the top end of the specimen. Then, the triaxial shear state was achieved by increasing the axial stress. The axial strain of the specimen was determined by the displacement of the nodes at the top end of the specimen and the axial stress by the reaction force of the same nodes. The radial strain of the specimen was determined by the displacement of the node located at the radial end on the mid plane at one-half of the height of the specimen, and the radial stress was determined from the confinement pressure. A commercial finite element package (LS-DYNA) was used for the analysis. The sign convention in the present study is positive for compression and negative for tension.

For the numerical implementation of the SCF model in the finite element analysis, the parameters shown in Table 1 [13] for Cuddeback lake soil were used. Rubber membrane was treated as an elastic material with an elastic modulus of 2900.8 psi (20 MPa) and a Poisson ratio of 0.5.

Results and discussion. The stress-strain curves of the triaxial tests at varying confinement pressure were generated numerically herein by using the set of the SCF model parameters shown in Table 1 [13], and the results are shown in Fig. 2. In order to assist the comparison of the simulation cases at varying confinement pressures, the range of the ordinate scale in each diagram is set to be the same (the range of 40 psi, i.e. 275.8 kPa).

Table 1. Parameters of the soil and crushable foam model [13] used for simulation in the present study

Category	Parameters		
Yield Surface	$J_{2D} = 77.52 + 15.26p + 0.751p^2$ (in psi^2 unit) $J_{2D} = 3{,}685{,}120{,}808.8 + 105{,}214.0p + 0.751p^2$ (in Pa^2 unit)		
Pressure-true volume strain relation	True strain	p (psi)	p (kPa)
	0	0	0
	0.0089	30	206.8
	0.0104	35	241.3
	0.0120	40	275.8
	0.0138	45	310.3
	0.0155	50	344.7
	0.0190	60	413.7
	0.0226	70	482.6
	0.0263	80	551.6
	0.0291	87.8	605.4
Elastic Parameters	Shear modulus of 2,500 psi (17.2 MPa) for the loading part Bulk modulus of 3,360 psi (23.2 MPa) for the loading part		

In Fig. 2, the pressure dependency of the yield strength in the simulated curves is well represented, which is rendered by the pressure-dependency of the yield surface function of the SCF model, eq. (1). The simulated curve under the condition of uniform deformation of the soil specimen with no end restraint (ideal case) shows a typical elastic-perfectly plastic behavior, as the model dictates. However, the case with the end restraint results in a notable deviation from such behavior, and the degree of deviation is pressure-dependent.

Based on the examination of all of the simulated curves shown in Fig. 2, the case with the end restraint (solid line) does not result in a significant difference in the initial yield strength from that of the ideal case with no end restraint (dashed line). On a quantitative base, the case with the end restraint increases yield strength by only 0.46 ± 0.13 percent with reference to that of the ideal case, in the confinement pressure range of 2-80 psi (13.8-551.6 kPa).

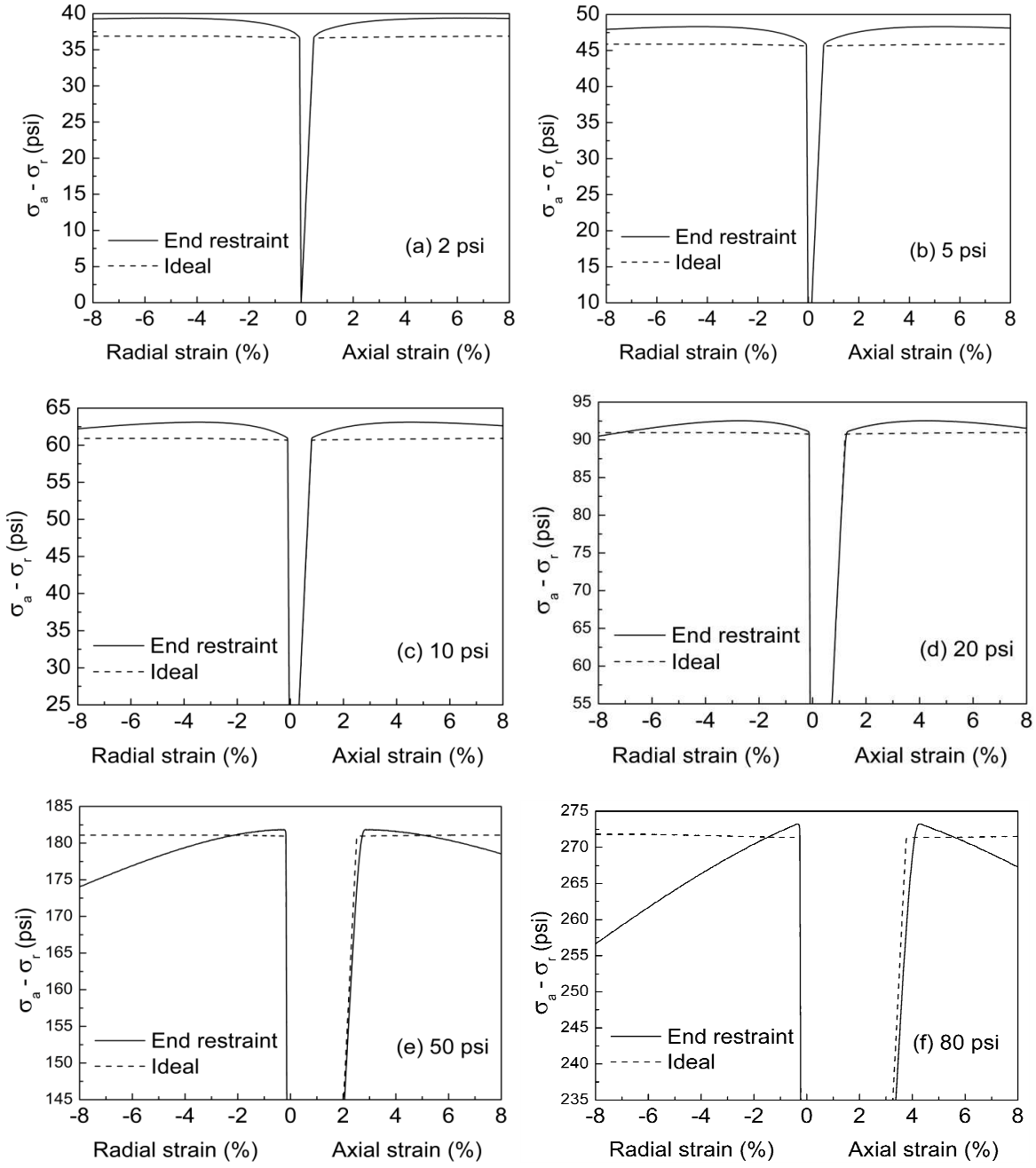

Fig. 2. Simulation results based on the soil and crushable foam model at the confinement pressures of (a) 2 psi (13.8 kPa), (b) 5 psi (34.5 kPa), (c) 10 psi (68.9 kPa), (d) 20 psi (137.9 kPa), (e) 50 psi (344.7 kPa), and (f) 80 psi (551.6 kPa) by using the parameter set shown in Table 1. σ_a is the axial stress and σ_r is the radial stress

Unlike yield strength, post-yield behavior was influenced notably by the end restraint, depending on the confinement pressure. In the simulation case with the end restraint, a notable strain hardening or strain softening transpires after initial yielding, unlike the ideal case with no end restraint. When the axial and radial strains are small, strain hardening generally occurs after initial yielding. As the strain increases further, peak stress appears, followed by strain softening thereafter. As the confinement pressure increases, peak stress materializes at lowered axial and radial strains, so that from the confinement pressure of 50 psi

(344.7 kPa), strain softening starts almost from the initial yielding. The yield strength now becomes the peak stress.

As the confinement pressure increases, the degree of strain hardening by the end restraint at the given axial and radial strains shows a decreasing trend.

By taking the sign of strain hardening as positive and that of strain softening as negative, on a quantitative base, the end restraint of the specimen causes strain hardening/softening of 7.46, 5.42, 3.24, 0.98, -1.32, and -1.50 percent with reference to the yield strength of the ideal case at 8 percent of axial strain, for the confinement pressures of 2 (13.8), 5 (34.5), 10 (68.9), 20 (137.9), 50 (344.7), and 80 (551.6) psi (kPa), respectively. At -8 percent of radial strain, the end restraint causes strain hardening/softening of 7.29, 5.04, 2.55, -0.27, -3.78, and -5.41 percent, respectively, with reference to the yield strength of the ideal case.

Neither the change in initial strength nor the post-yield behavior (confinement-pressure-dependent strain hardening or softening) due to the presence of the end restraint should be considered to represent the actual behavior of the soil in the triaxial test, which is not associated with the true material property. Thus, care needs to be taken to eliminate such artificial behavior in order to determine the true soil property from the triaxial stress-strain curve. As an extension of the current investigation, a more detailed analysis on the influence of non-uniform deformation on the triaxial stress-strain curve will be performed, which will include the comparison case with both the end restraint and rubber membrane. Also, a method to extract the true material parameters of the model via the comparison of the simulation cases will be investigated, and the results will be published elsewhere.

Conclusions. The stress-strain curve determined by a conventional triaxial test was simulated by a finite element method based on the displacement of the top and radial end points of the specimen. By employing a pressure-dependent and linearly elastic-perfectly plastic constitutive model, the effect of the end restraint on the determined stress-strain curve has been investigated. The end restraint slightly increases yield strength as compared to an ideal case with no end restraint. However, its influence is insignificant. It decreases the yield strength by only 0.46 ± 0.13 percent with reference to the ideal case with no end restraint, in the range of the confinement pressure of 2-80 psi (13.8-551.6 kPa).

Unlike yield strength, post-yield behavior is influenced notably by the end restraint, depending on the confinement pressure. When the axial and radial strains are small, strain hardening after initial yielding generally takes place. As the strain increases further, peak stress appears, followed by strain softening. As the confinement pressure increases, peak stress materializes at lowered axial and radial strains, so that from the confinement pressure of 50 psi (344.7 kPa), strain softening starts almost from the initial yielding. As the confinement pressure increases, the degrees of strain hardening by the end restraint at the given axial and radial strains show decreasing trends.

By taking the sign of strain hardening as positive and that of strain softening as negative, on a quantitative base, the end restraint of the specimen causes strain

hardening/softening of 7.46, 5.42, 3.24, 0.98, -1.32, and -1.50 percent with reference to the yield strength of ideal case at 8 percent of axial strain, for the confinement pressures of 2 (13.8), 5 (34.5), 10 (68.9), 20 (137.9), 50 (344.7), and 80 (551.6) psi (kPa), respectively. At -8 percent of radial strain, the end restraint causes strain hardening/softening of 7.29, 5.04, 2.55, -0.27, -3.78, and -5.41 percent, respectively, with reference to the yield strength of the ideal case. The change in initial strength and the artificial post-yield behavior (confinement-pressure-dependent strain hardening or softening) due to the presence of the end restraint need to be eliminated in order to determine the true soil property from the triaxial stress-strain curve.

Literature

1. Bishop, A.W. The Measurement of Soil Properties in the Triaxial Test / A.W. Bishop, D.J. Henkel. – London and Beccles: 2nd ed. William Clowes and Sons, Limited, 1962. – 28 p.

2. Schanz, T. The influence of geometry and end restraint on the strength in triaxial compression in numerical simulation / T. Schanz, P. Gussman // Numerical Methods in Geothechical Engineering, Smith, I.M. (Ed.). – Balkema, Ritterdam, 1994. – P. 129 –133.

3. Effects of end restraint and strain rate in triaxial tests / D. Sheng, B. Westerberg, H. Mattson, K. Axelsson // Comput. Geotech. – 21(3). – 1997. – P. 163 – 182.

4. Yang, Q. Numerical analysis of end effect in triaxial tests on clay / Q. Yang, J. Ge. – Elect. J. Geotech. Eng. – 17. – 2012. – P. 699 – 707.

5. Kreig, R.D. A Simple Constitutive Description for Cellular Concrete. Report No. SC-DR-72-0883, Sandia National Laboratories, Albuquerque, NM, 1972.

6. Swenson, D.V. A finite element model for the analysis of tailored pulse stimulation of bore holes / D.V. Swenson, L.M. Taylor // J. Numer. Anal. Methods in Geomech. – 7. – 1983. – P. 469 – 484.

7. Schwer, L. Laboratory Tests for Characterizing Geomaterials / L. Schwer // Engineering & Consulting Services, Livermore, CA, 2001. – P. 9 – 12.

8. Modeling mine blast with SPH / M.A. Barsotti, J.M.H. Puryear, D.J. Stevens, R.M. Alberson, P. McMahon // 12th International LS-DYNA Users Conference, Blast/Impact (1), 2012. – P. 1 – 11.

9. Finite element simulation of cone penetration / Jr. W.A. Foster, C.E. Johnson, R.C. Chiroux, T.R. Way // Appl. Math. Comput. 162, 2005. – P.735 – 749.

10. Johnson, J.B. Interpretation of the stress histories from shock impact tests on snow using embedded stress gauges / J.B. Johnson, J.A. Brown, E.S. Gaffney // Proceedings of the American Physical Society Topical Conference on Shock Compression of Condensed Matter, August 14-17, Albuquerque, New Mexico, Elsevier Science Publishers, 1990. – P. 117 – 120.

11. Hallquist, J.O. LS-DYNA Theory Manual, Livermore Software Technology Corporation / J.O. Hallquist. – Livermore, CA, 2006. – 150 p.

12. The MacNeal-Schwendler Corporation. MSC/DYTRAN Theory Manual, The MacNeal-Schwendler Corporation. Santa Ana, CA, 2010. – 70 p.

13. Constitutive Soil Properties for Cuddeback Lake, California and Carson Sink, Nevada / M.A. Thomas, D.E. Chitty, M.L. Gildea, C. T'Kindt. – Report No. NASA/CR-2008-215345, Langley Research Center, National Aeronautics and Space Administration, Hampton, VA, 2008. – 70 p.

Надійшла до редакції 23.09.2013